J/ψ AND Υ INCLUSIVE PHOTOPRODUCTION AT NEXT-TO-LEADING-ORDER

Yelyzaveta Yedelkina

Carlo Flore, Jean-Philippe Lansberg, Hua-Sheng Shao, Alice Colpani Serri, Yu Feng, Melih A. Ozcelik in IJCLab (Orsay)

October 29, 2021

French-Ukrainian Workshop
Instrumentation developments for High energy physics
27-29 October 2021, IJCLab, Paris-Saclay University

This project is supported by the European Union's Horizon 2020 research and innovation programme under Grant agreement no. 824093

Part I

Introducing inclusive J/ψ & Υ photoproduction

Introduction: inclusive $J/\psi(\Upsilon)$ photoproduction

C.-H. Chang, NPB172, 425 (1980); R. Baier & R. Rückl Z. Phys. C 19, 251(1983);

- as a reminder, J/ψ (Υ) is a $c\bar{c}$ ($b\bar{b}$) bound state with $J = 1,\ L = 0,\ S = 1$; vector particle

Introduction: inclusive $J/\psi(\Upsilon)$ photoproduction

C.-H. Chang, NPB172, 425 (1980); R. Baier & R. Rückl Z. Phys. C 19, 251(1983);

- as a reminder, J/ψ (Υ) is a $c\bar{c}$ ($b\bar{b}$) bound state with $J = 1,\ L = 0,\ S = 1$; vector particle
- inclusive photoproduction:

$$\gamma(Q^2 \simeq 0) + p \to J/\psi + X;$$

Introduction: inclusive $J/\psi(\Upsilon)$ photoproduction

C.-H. Chang, NPB172, 425 (1980); R. Baier & R. Rückl Z. Phys. C 19, 251(1983);

- as a reminder, J/ψ (Υ) is a $c\bar{c}$ ($b\bar{b}$) bound state with $J = 1,\ L = 0,\ S = 1$; vector particle
- inclusive photoproduction:

$$\gamma(Q^2 \simeq 0) + p \to J/\psi + X;$$

- We will discuss the photoproduction at NLO;

Introduction: inclusive $J/\psi(\Upsilon)$ photoproduction

C.-H. Chang, NPB172, 425 (1980); R. Baier & R. Rückl Z. Phys. C 19, 251(1983);

- as a reminder, $J/\psi\ (\Upsilon)$ is a $c\bar{c}$ ($b\bar{b}$) bound state with $J = 1,\ L = 0,\ S = 1$; vector particle
- inclusive photoproduction:

$$\gamma(Q^2 \simeq 0) + p \to J/\psi + X;$$

- We will discuss the photoproduction at NLO;
- 3 common models (differences in the treatment of the hadronisation):
  - Colour Singlet Model;
  - NRQCD and Colour Octet Mechanism;
  - Colour Evaporation Model;

see talk by K.Lynch

Basic pQCD approach: the Colour Singlet Model (CSM)

C.-H. Chang, NPB172, 425 (1980); R. Baier & R. Rückl Z. Phys. C 19, 251(1983);

One supposes two **factorisations**:

1. **collinear**, in which the hadronic cross section can be written as the convolution of the **PDFs** with the **partonic cross section**;

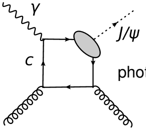

LO J/ψ photoproduction graph

Basic pQCD approach: the Colour Singlet Model (CSM)

C.-H. Chang, NPB172, 425 (1980); R. Baier & R. Rückl Z. Phys. C 19, 251(1983);

One supposes two **factorisations**:

1. **collinear**, in which the hadronic cross section can be written as the convolution of the **PDFs** with the **partonic cross section**;
2. between the hard part (a perturbative amplitude, which describes the $Q\bar{Q}$ **pair production**) and the soft part (a non-perturbative matrix element, which describes **hadronisation**):

- Perturbative creation of 2 quarks, Q and $\bar{Q}$

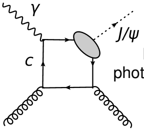

LO J/ψ photoproduction graph

- Non-perturbative binding of quarks

Basic pQCD approach: the Colour Singlet Model (CSM)

C.-H. Chang, NPB172, 425 (1980); R. Baier & R. Rückl Z. Phys. C 19, 251(1983);

One supposes two **factorisations**:

1. **collinear**, in which the hadronic cross section can be written as the convolution of the **PDFs** with the **partonic cross section**;
2. between the hard part (a perturbative amplitude, which describes the $Q\bar{Q}$ **pair production**) and the soft part (a non-perturbative matrix element, which describes **hadronisation**):

- Perturbative creation of 2 quarks, Q and $\bar{Q}$
  - on-shell
  - in a colour singlet state
  - with a vanishing relative momentum
  - in a ${}^3S_1$ state (for J/ψ, ψ' and Υ)
- Non-perturbative binding of quarks

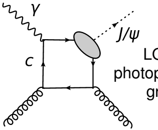

LO J/ψ photoproduction graph

Basic pQCD approach: the Colour Singlet Model (CSM)

C.-H. Chang, NPB172, 425 (1980); R. Baier & R. Rückl Z. Phys. C 19, 251(1983);

One supposes two **factorisations**:

1. **collinear**, in which the hadronic cross section can be written as the convolution of the **PDFs** with the **partonic cross section**;
2. between the hard part (a perturbative amplitude, which describes the $Q\bar{Q}$ **pair production**) and the soft part (a non-perturbative matrix element, which describes **hadronisation**):

- Perturbative creation of 2 quarks, Q and $\bar{Q}$
  - on-shell
  - in a colour singlet state
  - with a vanishing relative momentum
  - in a $^3S_1$ state (for J/ψ, ψ' and Υ)
- Non-perturbative binding of quarks
  $\rightarrow$ Schrödinger wave function at $r = 0$

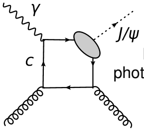

LO J/ψ photoproduction graph

Basic pQCD approach: the Colour Singlet Model (CSM)

C.-H. Chang, NPB172, 425 (1980); R. Baier & R. Rückl Z. Phys. C 19, 251(1983);

One supposes two **factorisations**:

1. **collinear**, in which the hadronic cross section can be written as the convolution of the **PDFs** with the **partonic cross section**;
2. between the hard part (a perturbative amplitude, which describes the $Q\bar{Q}$ **pair production**) and the soft part (a non-perturbative matrix element, which describes **hadronisation**):

- Perturbative creation of 2 quarks, Q and $\bar{Q}$
  - on-shell
  - in a colour singlet state
  - with a vanishing relative momentum
  - in a $^3S_1$ state (for J/ψ, ψ' and Υ)
- Non-perturbative binding of quarks
  $\rightarrow$ Schrödinger wave function at $r = 0$

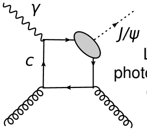

LO J/ψ photoproduction graph

CSM: the Taylor series expansion of the amplitude in the $\overline{QQ}$ relative momentum (v) to the first non-vanishing (Leading-v NRQCD) term.

General structure of NLO corrections

Singularities at NLO [and how they are removed]:

General structure of NLO corrections

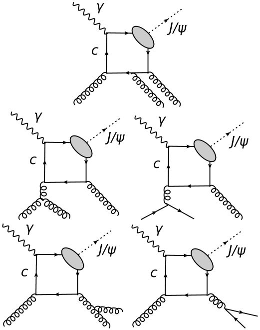

Singularities at NLO [and how they are removed]:

- Real emission
  - Infrared divergences: Soft [cancelled by loop IR contr. after phase-space integration (the KLN theorem)]
  - Infrared divergences: Collinear

[The quark and antiquark attached to the ellipsis are taken as on-shell and their relative velocity v is set to zero.]

General structure of NLO corrections

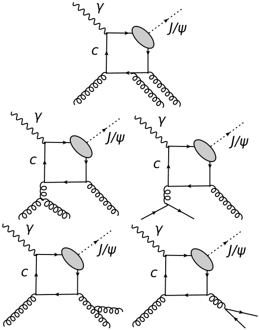

Singularities at NLO [and how they are removed]:

- Real emission
  - Infrared divergences: Soft [cancelled by loop IR contr. after phase-space integration (the KLN theorem)]
  - Infrared divergences: Collinear
    - ★ initial emission [subtracted by Altarelli-Parisi counter-terms (AP-CT) in the factorised PDFs]
    - ★ final emission [cancelled by loop Infrared contribution after phase-space integration (the KLN theorem)]

[The quark and antiquark attached to the ellipsis are taken as on-shell and their relative velocity v is set to zero.]

General structure of NLO corrections

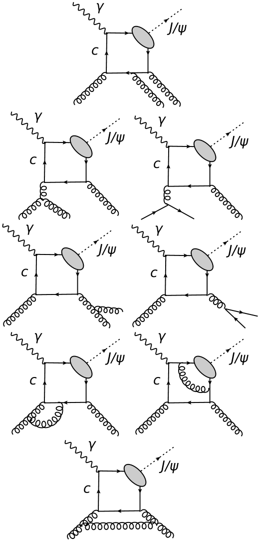

Singularities at NLO [and how they are removed]:

- Real emission
  - Infrared divergences: Soft [cancelled by loop IR contr. after phase-space integration (the KLN theorem)]
  - Infrared divergences: Collinear
    - ★ initial emission [subtracted by Altarelli-Parisi counter-terms (AP-CT) in the factorised PDFs]
    - ★ final emission [cancelled by loop Infrared contribution after phase-space integration (the KLN theorem)]
- Virtual (loop) contribution

[The quark and antiquark attached to the ellipsis are taken as on-shell and their relative velocity v is set to zero.]

General structure of NLO corrections

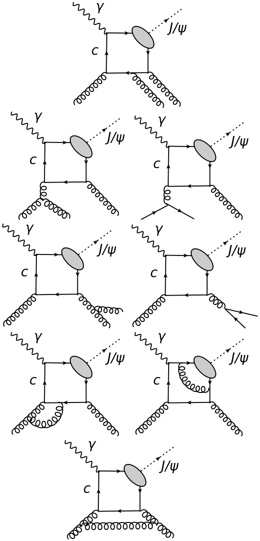

Singularities at NLO [and how they are removed]:

- Real emission
  - Infrared divergences: Soft [cancelled by loop IR contr. after phase-space integration (the KLN theorem)]
  - Infrared divergences: Collinear
    - ★ initial emission [subtracted by Altarelli-Parisi counter-terms (AP-CT) in the factorised PDFs]
    - ★ final emission [cancelled by loop Infrared contribution after phase-space integration (the KLN theorem)]
- Virtual (loop) contribution
  - Ultraviolet divergences: [removed by renormalisation]
  - Infrared divergences: [cancelled by real Infrared contribution]

[The quark and antiquark attached to the ellipsis are taken as on-shell and their relative velocity v is set to zero.]

Part II

Photoproduction at mid and high P_T at HERA

Different contributions in the CSM up to NLO

C. Flore, J.P. Lansberg, H.S. Shao, YY, PLB 811 (2020) 135926

Different contributions in the CSM up to NLO

C. Flore, J.P. Lansberg, H.S. Shao, YY, PLB 811 (2020) 135926

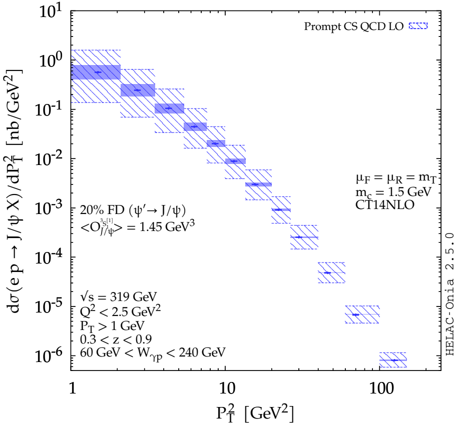

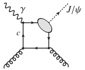

$$\gamma + g \to \psi + g \; @ \; \alpha\alpha_s^2$$

Notes:
All the computations were done with HELAC-ONIA. The scale and mass uncertainties are shown by the hatched and solid bands. **H.S. Shao, CPC198 (2016) 238**; See also `https://nloaccess.in2p3.fr`

[The quark and antiquark attached to the ellipsis are taken as on-shell and their relative velocity v is set to zero.]

Different contributions in the CSM up to NLO

C. Flore, J.P. Lansberg, H.S. Shao, YY, PLB 811 (2020) 135926

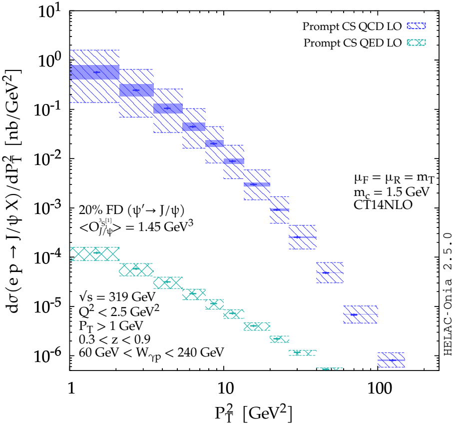

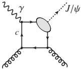

$\gamma + g \to \psi + g$ @ $\alpha\alpha_s^2$

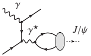

$\gamma + q \to \psi + q$ @ α^3 [NEW !]

Notes:
All the computations were done with HELAC-ONIA. The scale and mass uncertainties are shown by the hatched and solid bands. **H.S. Shao, CPC198 (2016) 238**; See also `https://nloaccess.in2p3.fr`
[The quark and antiquark attached to the ellipsis are taken as on-shell and their relative velocity v is set to zero.]

Different contributions in the CSM up to NLO

C. Flore, J.P. Lansberg, H.S. Shao, YY, PLB 811 (2020) 135926

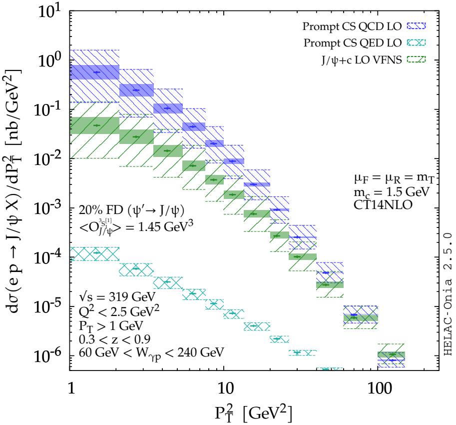

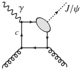

$\gamma + g \to \psi + g$ @ $\alpha\alpha_s^2$

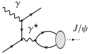

$\gamma + q \to \psi + q$ @ α^3 [NEW !]

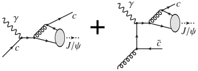

$\gamma + c \to \psi + c$ @ $\alpha\alpha_s^2$ w. 4 Flavour Scheme

$\gamma + g \to \psi + c + \bar{c}$ @ $\alpha\alpha_s^3$ w. 3 Flavour Scheme

VFNS [also NEW !]

Notes:
All the computations were done with HELAC-ONIA. The scale and mass uncertainties are shown by the hatched and solid bands. **H.S. Shao, CPC198 (2016) 238**; See also `https://nloaccess.in2p3.fr`

[The quark and antiquark attached to the ellipsis are taken as on-shell and their relative velocity v is set to zero.]

Different contributions in the CSM up to NLO

C. Flore, J.P. Lansberg, H.S. Shao, YY, PLB 811 (2020) 135926

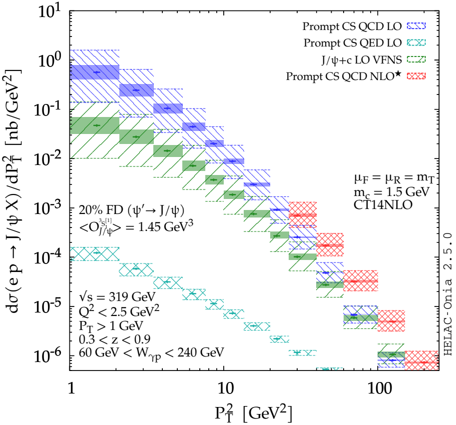

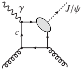

$\gamma + g \to \psi + g$ @ $\alpha\alpha_s^2$

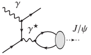

$\gamma + q \to \psi + q$ @ α^3 [NEW !]

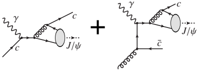

$$\begin{cases} \gamma+c\to\psi+c \text{ @ } \alpha\alpha_s^2 \text{ w. 4 Flavour Scheme} \\ \gamma+g\to\psi+c+\bar{c} \text{ @ } \alpha\alpha_s^3 \text{ w. 3 Flavour Scheme} \end{cases}$$

VFNS [also NEW !]

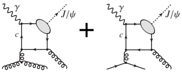

$$\begin{cases} \gamma+g\to\psi+g+g \text{ @ } \alpha\alpha_s^3 \\ \gamma+q\to\psi+g+q \text{ @ } \alpha\alpha_s^3 \end{cases}$$

$[+\ \gamma + g \to \psi + g]$

Notes:
All the computations were done with HELAC-ONIA. The scale and mass uncertainties are shown by the hatched and solid bands. **H.S. Shao, CPC198 (2016) 238**; See also `https://nloaccess.in2p3.fr`

[The quark and antiquark attached to the ellipsis are taken as on-shell and their relative velocity v is set to zero.]

NLO* only contains the real-emission contributions with an IR cut-off and is expected to account for the leading P_T contributions at NLO (P_T^{-6}). It has been succesfully checked against full NLO computations for $P_T > 3$ GeV.

Comparison to the latest HERA data by H1

C.Flore, JP Lansberg, H.S. Shao, YY, PLB 811 (2020) 135926

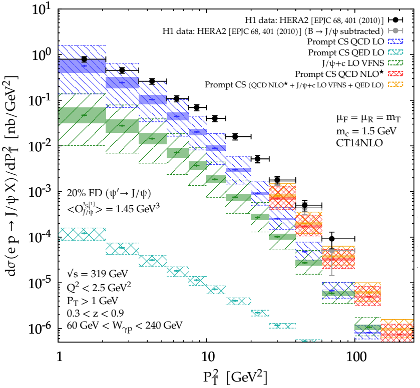

Comparison to the latest HERA data by H1

C.Flore, JP Lansberg, H.S. Shao, YY, PLB 811 (2020) 135926

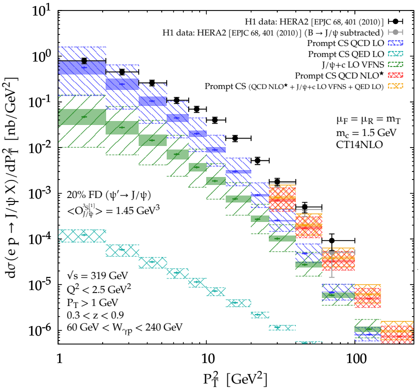

- LO QCD : OK at low P_T

Comparison to the latest HERA data by H1

C.Flore, JP Lansberg, H.S. Shao, YY, PLB 811 (2020) 135926

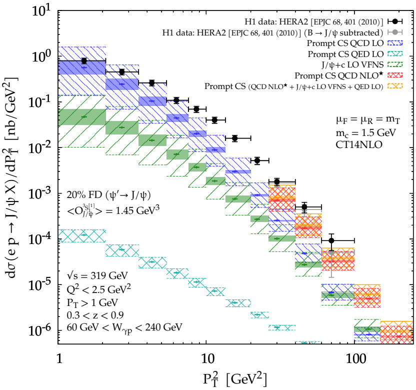

- LO QCD : OK at low P_T
- LO QED small but much harder

Comparison to the latest HERA data by H1

C.Flore, JP Lansberg, H.S. Shao, YY, PLB 811 (2020) 135926

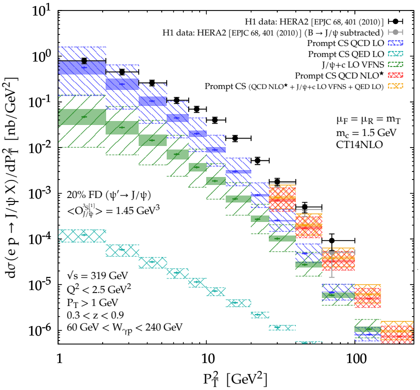

- LO QCD : OK at low P_T
- LO QED small but much harder
- J/ψ+charm: matter at high P_T

Comparison to the latest HERA data by H1

C.Flore, JP Lansberg, H.S. Shao, YY, PLB 811 (2020) 135926

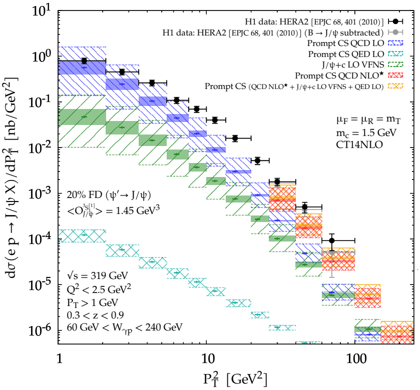

- LO QCD : OK at low P_T
- LO QED small but much harder
- J/ψ+charm: matter at high P_T
- NLO$^{(\star)}$ close the data, the overall sum nearly agrees with them

Comparison to the latest HERA data by H1

C.Flore, JP Lansberg, H.S. Shao, YY, PLB 811 (2020) 135926

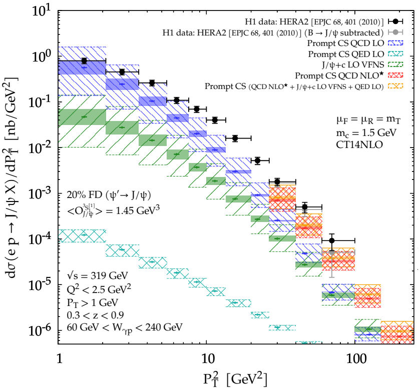

- LO QCD : OK at low P_T
- LO QED small but much harder
- J/ψ+charm: matter at high P_T
- NLO$^{(\star)}$ close the data, the overall sum nearly agrees with them
- Agreement with the last bin when the expected $B \to J/\psi$ feed down (in gray) is subtracted

Comparison to the latest HERA data by H1

C.Flore, JP Lansberg, H.S. Shao, YY, PLB 811 (2020) 135926

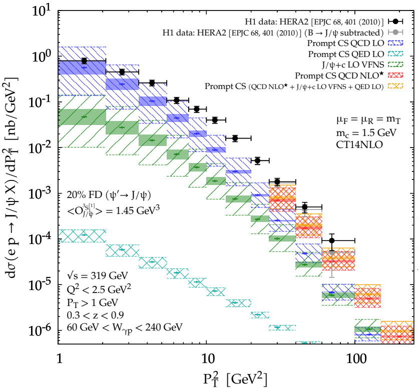

- LO QCD : OK at low P_T
- LO QED small but much harder
- J/ψ+charm: matter at high P_T
- NLO$^{(\star)}$ close the data, the overall sum nearly agrees with them
- Agreement with the last bin when the expected $B \to J/\psi$ feed down (in gray) is subtracted

The CSM up to $\alpha\alpha_s^3$ reproduces photoproduction at HERA

$\rightarrow$ we will restrict to CSM for our EIC predictions

Part III

Photoproduction at mid and high P_T at the Electron-Ion Collider

Predictions for the EIC : $J/\psi + X$ ($\sqrt{s_{ep}} = 45$ GeV)

C. Flore, J.P. Lansberg, H.S. Shao, YY, PLB 811 (2020) 135926

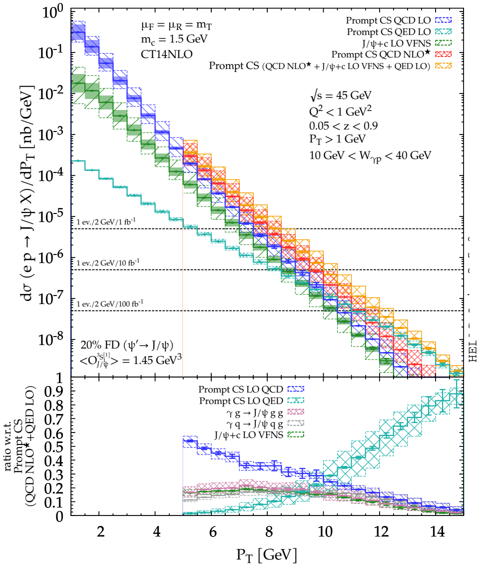

- At $\sqrt{s_{ep}} = 45$ GeV, one gets into valence region

Predictions for the EIC : $J/\psi + X$ ($\sqrt{s_{ep}} = 45$ GeV)

C. Flore, J.P. Lansberg, H.S. Shao, YY, PLB 811 (2020) 135926

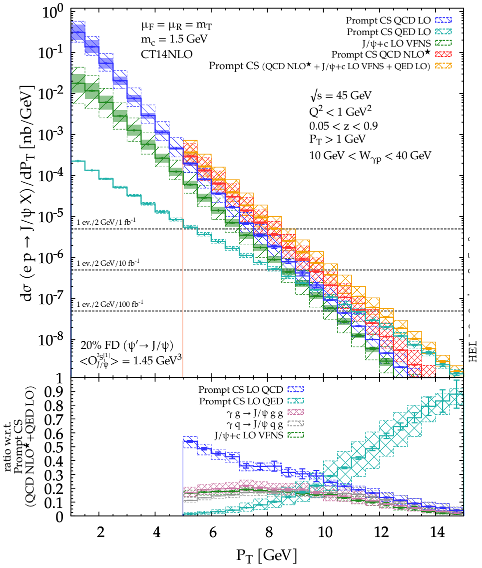

- At $\sqrt{s_{ep}} = 45$ GeV, one gets into valence region
- Yield steeply falling with P_T
- Yield can be measured up to $P_T \sim 11$ GeV with $\mathcal{L} = 100$ fb^{-1}

[using both *ee* and $\mu\mu$ decay channels and $\varepsilon_{J/\psi} \simeq 80\%$]

Predictions for the EIC : $J/\psi + X$ ($\sqrt{s_{ep}} = 45$ GeV)

C. Flore, J.P. Lansberg, H.S. Shao, YY, PLB 811 (2020) 135926

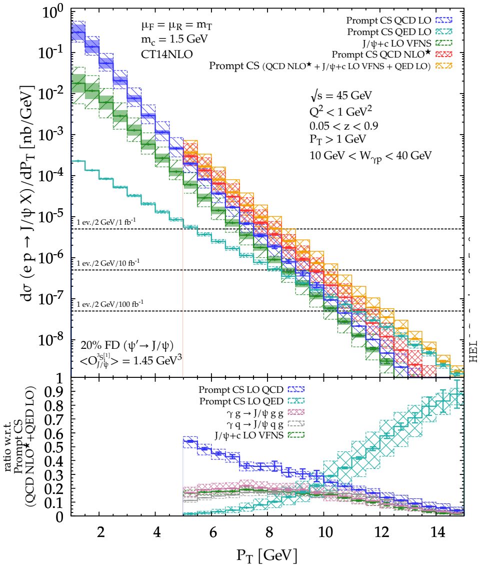

- At $\sqrt{s_{ep}} = 45$ GeV, one gets into valence region
- Yield steeply falling with P_T
- Yield can be measured up to $P_T \sim 11$ GeV with $\mathcal{L} = 100$ fb^{-1}

  [using both *ee* and $\mu\mu$ decay channels and $\varepsilon_{J/\psi} \simeq 80\%$]
- QED contribution leading at the largest reachable P_T
- photon-quark fusion contributes more than 30 % for $P_T > 8$ GeV

Predictions for the EIC : $J/\psi + X$ ($\sqrt{s_{ep}} = 140$ GeV)

C. Flore, J.P. Lansberg, H.S. Shao, YY, PLB 811 (2020) 135926

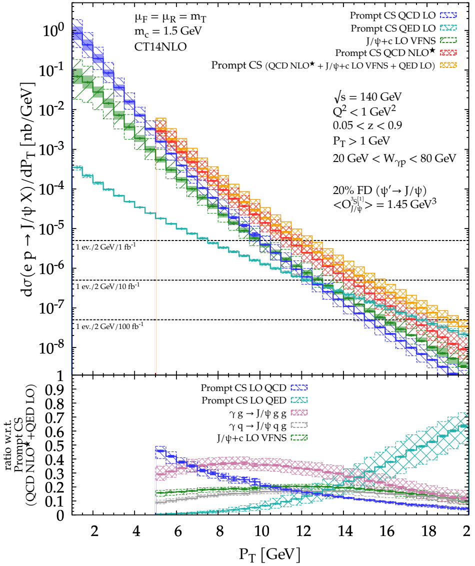

- At $\sqrt{s_{ep}} = 140$ GeV, larger P_T range up to approx. 18 GeV

Predictions for the EIC : $J/\psi + X$ ($\sqrt{s_{ep}} = 140$ GeV)

C. Flore, J.P. Lansberg, H.S. Shao, YY, PLB 811 (2020) 135926

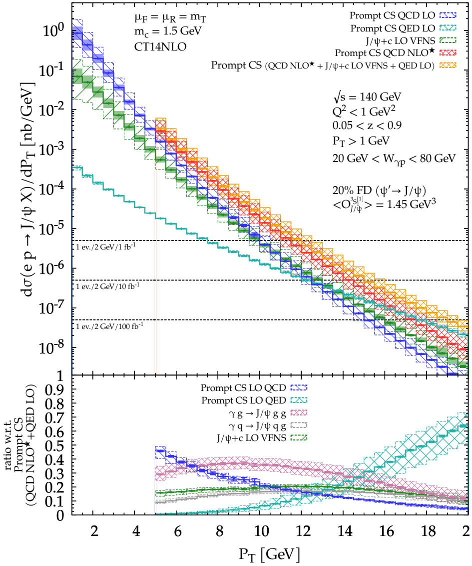

- At $\sqrt{s_{ep}} = 140$ GeV, larger P_T range up to approx. 18 GeV
- QED contribution also leading at the largest reachable P_T
- photon-gluon fusion contributions dominant up to approx. 15 GeV

Predictions for the EIC : $J/\psi + X$ ($\sqrt{s_{ep}} = 140$ GeV)

C. Flore, J.P. Lansberg, H.S. Shao, YY, PLB 811 (2020) 135926

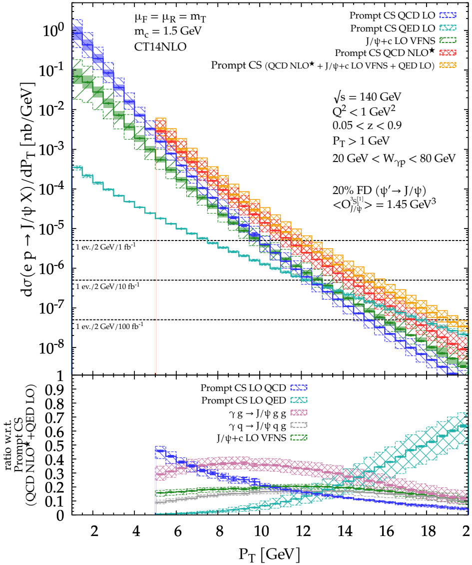

- At $\sqrt{s_{ep}} = 140$ GeV, larger P_T range up to approx. 18 GeV
- QED contribution also leading at the largest reachable P_T
- photon-gluon fusion contributions dominant up to approx. 15 GeV
- $J/\psi + 2$ hard partons [*i.e.* $J/\psi + \{gg, qg, c\bar{c}\}$] dominant for $P_T \sim 8 - 15$ GeV

Predictions for the EIC : $J/\psi + X$ ($\sqrt{s_{ep}} = 140$ GeV)

C. Flore, J.P. Lansberg, H.S. Shao, YY, PLB 811 (2020) 135926

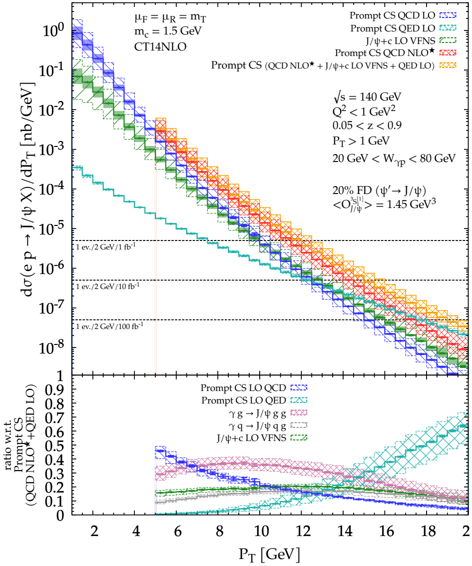

- At $\sqrt{s_{ep}} = 140$ GeV, larger P_T range up to approx. 18 GeV
- QED contribution also leading at the largest reachable P_T
- photon-gluon fusion contributions dominant up to approx. 15 GeV
- $J/\psi + 2$ hard partons [*i.e.* $J/\psi + \{gg, qg, c\bar{c}\}$] dominant for $P_T \sim 8 - 15$ GeV
- It could lead to the observation of $J/\psi + 2$ jets with moderate $P_T^{\rm jet}$

Predictions for the EIC : $J/\psi + X$ ($\sqrt{s_{ep}} = 140$ GeV)

C. Flore, J.P. Lansberg, H.S. Shao, YY, PLB 811 (2020) 135926

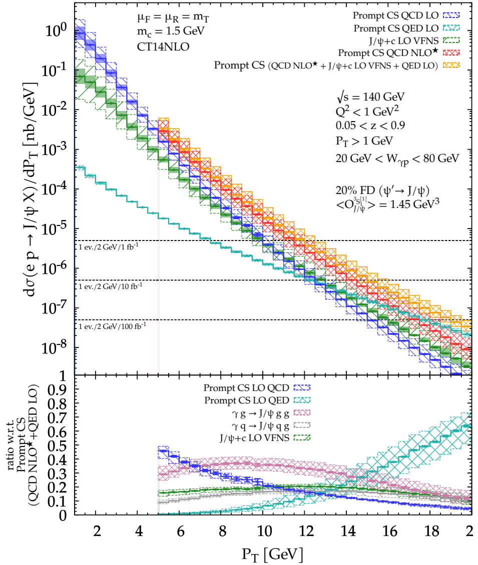

- At $\sqrt{s_{ep}} = 140$ GeV, larger P_T range up to approx. 18 GeV
- QED contribution also leading at the largest reachable P_T
- photon-gluon fusion contributions dominant up to approx. 15 GeV
- $J/\psi + 2$ hard partons [*i.e.* $J/\psi + \{gg, qg, c\bar{c}\}$] dominant for $P_T \sim 8 - 15$ GeV
- It could lead to the observation of $J/\psi + 2$ jets with moderate P_T^{jet}
- with a specific topology where the leading jet$_1$ recoils on the $J/\psi+$ jet$_2$ pair

Predictions for the EIC : $J/\psi + X$ ($\sqrt{s_{ep}} = 140$ GeV)

C. Flore, J.P. Lansberg, H.S. Shao, YY, PLB 811 (2020) 135926

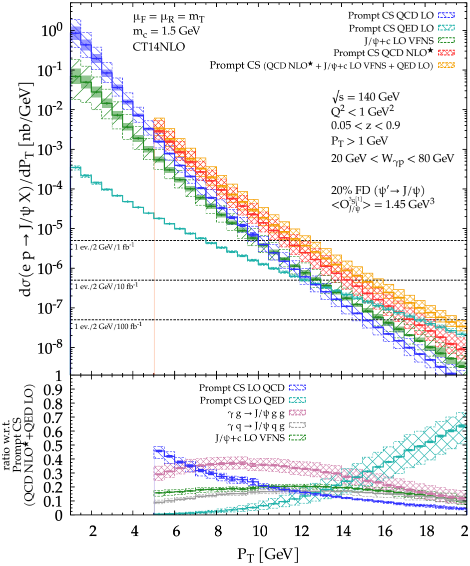

- At $\sqrt{s_{ep}} = 140$ GeV, larger P_T range up to approx. 18 GeV
- QED contribution also leading at the largest reachable P_T
- photon-gluon fusion contributions dominant up to approx. 15 GeV
- $J/\psi + 2$ hard partons [*i.e.* $J/\psi + \{gg, qg, c\bar{c}\}$] dominant for $P_T \sim 8 - 15$ GeV
- It could lead to the observation of $J/\psi + 2$ jets with moderate P_T^{jet}
- with a specific topology where the leading jet$_1$ recoils on the $J/\psi+$ jet$_2$ pair
- We expect the $d\sigma$ to vanish when $E_{\text{jet}_2}^{J/\psi \text{ rest fr.}} \to 0$

Part IV

Study of the impact of the NLO corrections to P_T-integrated cross section

The negative cross-sections issue at high energies

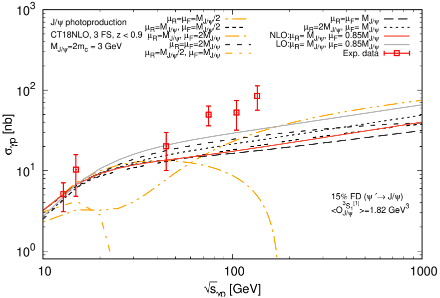

Exp. data: H1 - M.Kraemer: NPB 459(1996)3-50, FTPS - B.H.Denby et al.: PRL 52(1984)795-798, NAI - NA14Collaboration, R.Barate et al.:Z.Phys.C 33(1987)505

The negative cross-sections issue at high energies

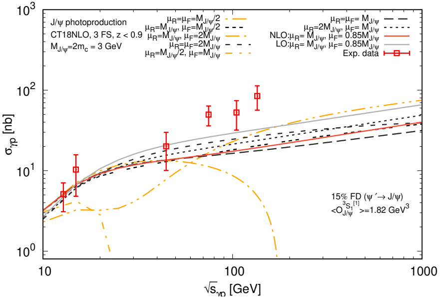

- NLO cross section for J/ψ photoproduction becomes negative for large μ_F when $\sqrt{s_{\gamma p}}$ increases

Exp. data: H1 - M.Kraemer: NPB 459(1996)3-50, FTPS - B.H.Denby et al.: PRL 52(1984)795-798, NAI - NA14Collaboration, R.Barate et al.:Z.Phys.C 33(1987)505

The negative cross-sections issue at high energies

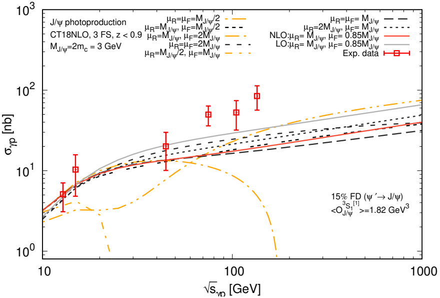

- NLO cross section for J/ψ photoproduction becomes negative for large μ_F when $\sqrt{s_{\gamma p}}$ increases
- For $\mu_F = 2M$, $\sigma < 0$ as in case of η_c hadroproduction

J.P. Lansberg, M.A. Ozcelik: Eur.Phys.J.C 81 (2021) 6, 497

Exp. data: H1 - M.Kraemer: NPB 459(1996)3-50, FTPS - B.H.Denby et al.: PRL 52(1984)795-798, NAI - NA14Collaboration, R.Barate et al.:Z.Phys.C 33(1987)505

The negative cross-sections issue at high energies

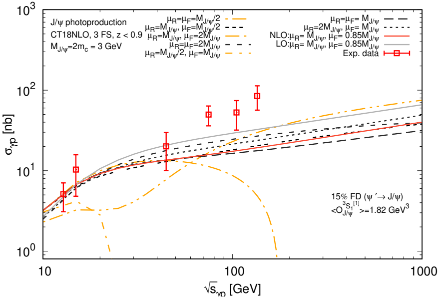

- NLO cross section for J/ψ photoproduction becomes negative for large μ_F when $\sqrt{s_{\gamma p}}$ increases
- For $\mu_F = 2M$, $\sigma < 0$ as in case of η_c hadroproduction

J.P. Lansberg, M.A. Ozcelik: Eur.Phys.J.C 81 (2021) 6, 497

- 2 possible sources of negative partonic cross sections: loop corrections (interference) and from real emission (subtraction of IR poles)

Exp. data: H1 - M.Kraemer: NPB 459(1996)3-50, FTPS - B.H.Denby et al.: PRL 52(1984)795-798, NAI - NA14Collaboration, R.Barate et al.:Z.Phys.C 33(1987)505

Negative cross-section values

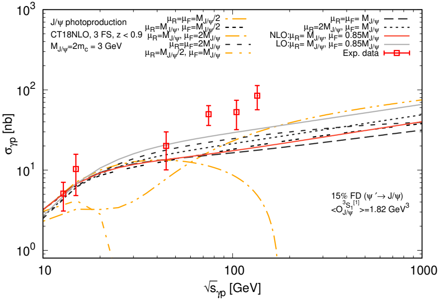

- Initial state collinear divergences are removed via the subtraction into the PDFs via AP-CT

Negative cross-section values

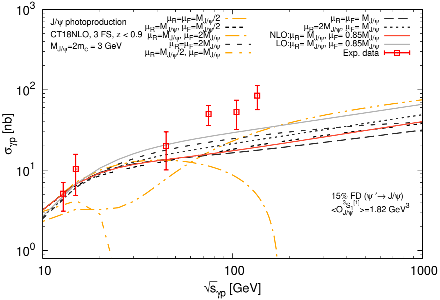

- Initial state collinear divergences are removed via the subtraction into the PDFs via AP-CT
- $\lim_{\hat{s}\to\infty} \hat{\sigma}^{NLO}_{\gamma i} \propto \left(\log \frac{m_Q^2}{{\mu_F}^2} + A_{\gamma i}\right)$, $A_{\gamma g} = A_{\gamma q}$

Negative cross-section values

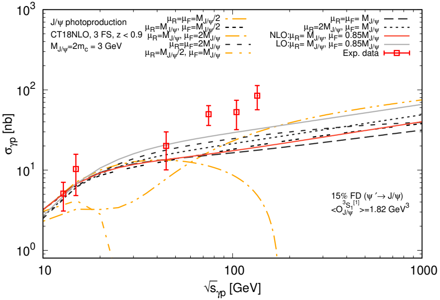

- Initial state collinear divergences are removed via the subtraction into the PDFs via AP-CT
- $\lim_{\hat{s}\to\infty} \hat{\sigma}^{NLO}_{\gamma i} \propto \left(\log \frac{m_Q^2}{{\mu_F}^2} + A_{\gamma i}\right)$, $A_{\gamma g} = A_{\gamma q}$
- If large $\mu_F \to \hat{\sigma} < 0 \to \sigma < 0$: over-subtraction from AP-CT into the PDFs

A scale prescription for μ_F

J.P. Lansberg, M.A. Ozcelik: Eur.Phys.J.C 81 (2021) 6, 497;

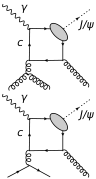

- In principle, such negative terms should be compensated by the evolution of the PDFs governed by the DGLAP equations;

A scale prescription for μ_F

J.P. Lansberg, M.A. Ozcelik: Eur.Phys.J.C 81 (2021) 6, 497;

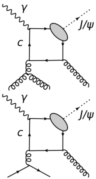

- In principle, such negative terms should be compensated by the evolution of the PDFs governed by the DGLAP equations;
- $A_{\gamma g}, A_{\gamma q}$ are process-dependent, while the DGLAP equations are process-independent, which makes the compensation imperfect;

A scale prescription for μ_F

J.P. Lansberg, M.A. Ozcelik: Eur.Phys.J.C 81 (2021) 6, 497;

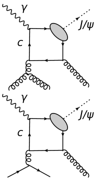

- In principle, such negative terms should be compensated by the evolution of the PDFs governed by the DGLAP equations;
- $A_{\gamma g}, A_{\gamma q}$ are process-dependent, while the DGLAP equations are process-independent, which makes the compensation imperfect;
- But as $A_{\gamma g} = A_{\gamma q}$, we can choose μ_F such that $\lim_{\hat{s}\to\infty} \hat{\sigma}_{\gamma i}^{NLO} = 0$

A scale prescription for μ_F

J.P. Lansberg, M.A. Ozcelik: Eur.Phys.J.C 81 (2021) 6, 497;

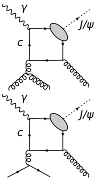

- In principle, such negative terms should be compensated by the evolution of the PDFs governed by the DGLAP equations;
- $A_{\gamma g}, A_{\gamma q}$ are process-dependent, while the DGLAP equations are process-independent, which makes the compensation imperfect;
- But as $A_{\gamma g} = A_{\gamma q}$, we can choose μ_F such that $\lim_{\hat{s}\to\infty} \hat{\sigma}_{\gamma i}^{NLO} = 0$
- This amounts to consider that all the QCD corrections are in the PDFs

A scale prescription for μ_F

J.P. Lansberg, M.A. Ozcelik: Eur.Phys.J.C 81 (2021) 6, 497;

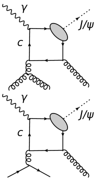

- In principle, such negative terms should be compensated by the evolution of the PDFs governed by the DGLAP equations;
- $A_{\gamma g}, A_{\gamma q}$ are process-dependent, while the DGLAP equations are process-independent, which makes the compensation imperfect;
- But as $A_{\gamma g} = A_{\gamma q}$, we can choose μ_F such that $\lim_{\hat{s}\to\infty} \hat{\sigma}^{NLO}_{\gamma i} = 0$
- This amounts to consider that all the QCD corrections are in the PDFs
- The choice of factorisation scale to avoid possible negative hadronic cross-section: (for $\eta_Q: \; A_{gi} = -1$) $\mu_F = \hat{\mu}_F = Me^{A_{\gamma i}/2}$;

A scale prescription for μ_F

J.P. Lansberg, M.A. Ozcelik: Eur.Phys.J.C 81 (2021) 6, 497;

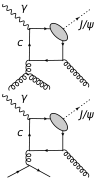

- In principle, such negative terms should be compensated by the evolution of the PDFs governed by the DGLAP equations;
- $A_{\gamma g}, A_{\gamma q}$ are process-dependent, while the DGLAP equations are process-independent, which makes the compensation imperfect;
- But as $A_{\gamma g} = A_{\gamma q}$, we can choose μ_F such that $\lim_{\hat{s}\to\infty} \hat{\sigma}^{NLO}_{\gamma i} = 0$
- This amounts to consider that all the QCD corrections are in the PDFs
- The choice of factorisation scale to avoid possible negative hadronic cross-section: (for $\eta_Q: \;\; A_{gi} = -1$) $\mu_F = \hat{\mu}_F = Me^{A_{\gamma i}/2}$;
- For J/ψ (Υ) photoproduction: $\hat{\mu}_F = 0.85M$ $(P_T \in [0, \infty],\;\; z < 0.9)$

Results with $\hat{\mu}_F = 0.85M$

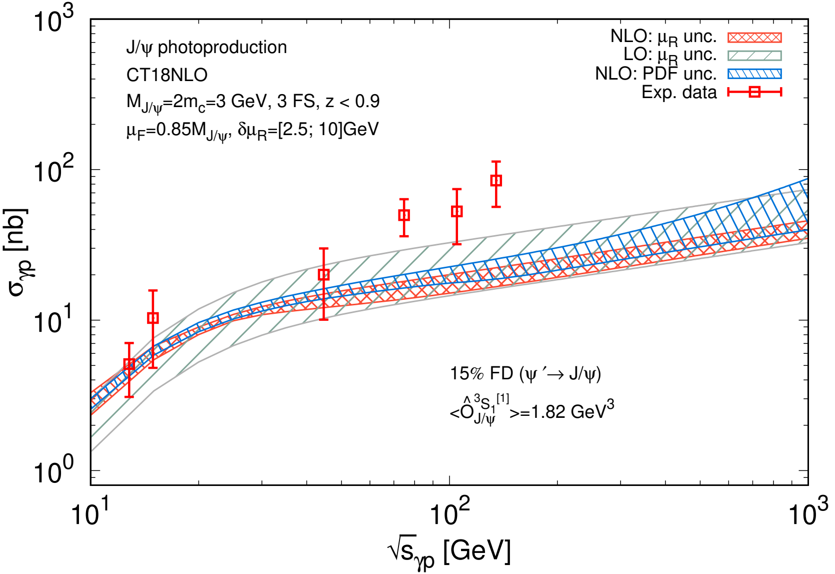

Exp. data: H1 - M.Kraemer: Nucl.Phys.B 459(1996)3-50, FTPS - B.H.Denbyet al.: Phys.Rev.Lett. 52(1984)795-798, NAI - NA14Collaboration, R.Barateet al.:Z.Phys.C 33(1987)505

Part V

Can J/ψ & Υ allow us to probe PDFs? : PDF vs scale uncertainties

J/ψ: PDF uncertainties of $\sigma(\sqrt{s_{\gamma p}})$

- PDF uncertainties increase at large $\sqrt{s}$ (i.e. small x);

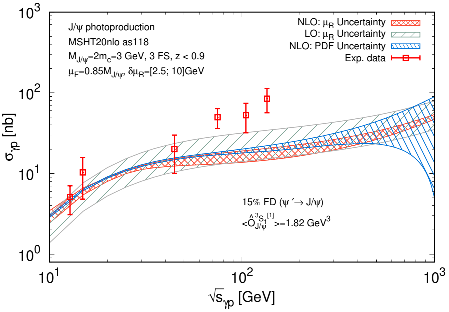

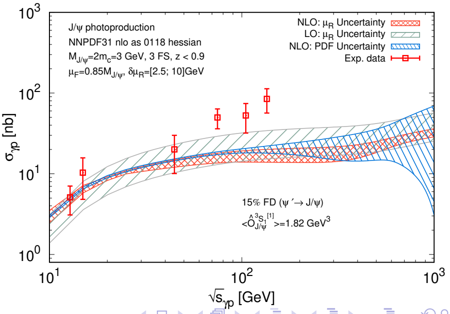

J/ψ: PDF uncertainties of $\sigma(\sqrt{s_{\gamma p}})$

- PDF uncertainties increase at large $\sqrt{s}$ (i.e. small x);
- The μ_R unc. are reduced at NLO in comparison with LO;

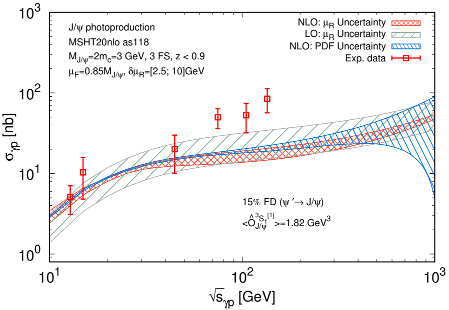

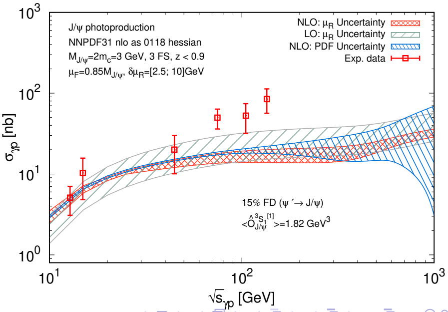

J/ψ: PDF uncertainties of $\sigma(\sqrt{s_{\gamma p}})$

- PDF uncertainties increase at large $\sqrt{s}$ (i.e. small x);
- The μ_R unc. are reduced at NLO in comparison with LO;
- An increase of μ_R unc. from $\sqrt{s_{\gamma p}} \gtrsim 50$GeV comes from (negative) loop corrections;

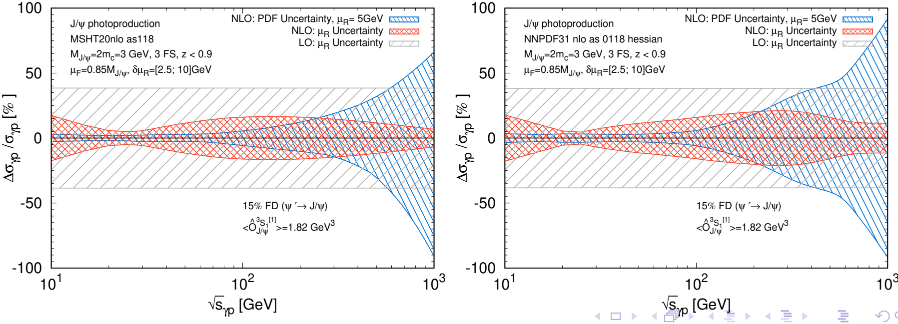

J/ψ: PDF uncertainties of $\sigma(\sqrt{s_{\gamma p}})$

- PDF uncertainties increase at large $\sqrt{s}$ (i.e. small x);
- The μ_R unc. are reduced at NLO in comparison with LO;
- An increase of μ_R unc. from $\sqrt{s_{\gamma p}} \gtrsim 50$GeV comes from (negative) loop corrections;
- At NNLO we will have such contributions squared;

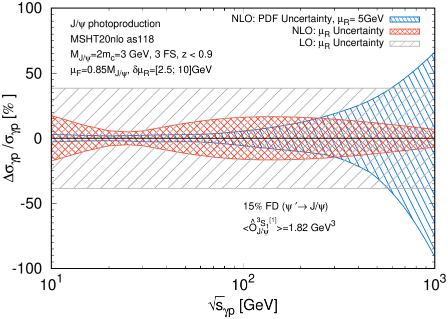

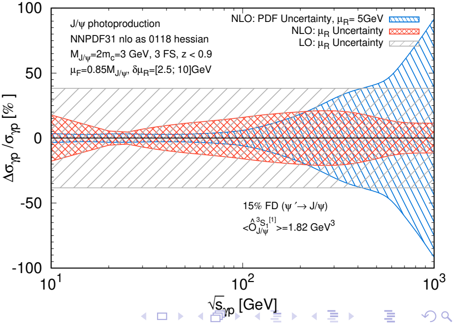

J/ψ: PDF uncertainties of $\sigma(\sqrt{s_{\gamma p}})$

- PDF uncertainties increase at large $\sqrt{s}$ (i.e. small x);
- The μ_R unc. are reduced at NLO in comparison with LO;
- An increase of μ_R unc. from $\sqrt{s_{\gamma p}} \gtrsim$ 50GeV comes from (negative) loop corrections;
- At NNLO we will have such contributions squared;
- Likely positive NNLO corrections beside a further reduction of the μ_R unc.

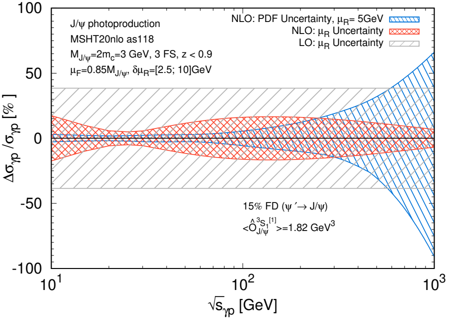

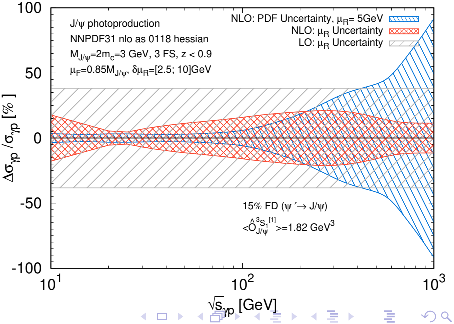

$\sigma_{ep}(\sqrt{s})$

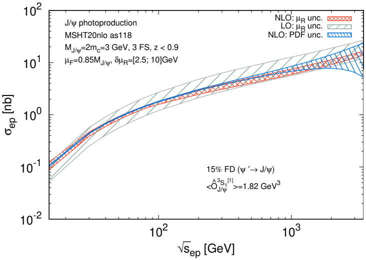

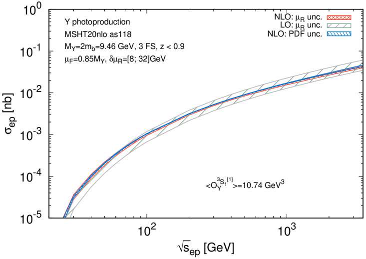

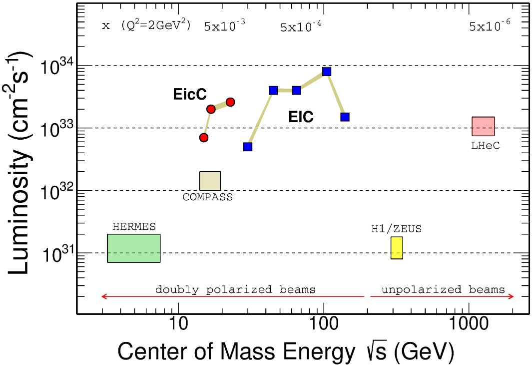

Possibility to constrain PDF at NNLO if μ_R unc. are further reduced

Part VI

Conclusions

Conclusions

- For quarkonium production, QCD corrections with P_T-enhanced topologies are known to be important: we have revisited J/ψ photoproduction at HERA

Conclusions

- For quarkonium production, QCD corrections with P_T-enhanced topologies are known to be important: we have revisited J/ψ photoproduction at HERA

- We have seen that CSM can describe the latest high-P_T HERA photoprod. data

Conclusions

- For quarkonium production, QCD corrections with P_T-enhanced topologies are known to be important: we have revisited J/ψ photoproduction at HERA
- We have seen that CSM can describe the latest high-P_T HERA photoprod. data
- $\sqrt{s_{ep}} = 140$ GeV,
  - gamma-quark QED contribution [new !] leading at high P_T
  - gluon-fusion mostly dominant
  - $J/\psi + 2$ jets accessible

Conclusions

- For quarkonium production, QCD corrections with P_T-enhanced topologies are known to be important: we have revisited J/ψ photoproduction at HERA

- We have seen that CSM can describe the latest high-P_T HERA photoprod. data
- $\sqrt{s_{ep}} = 140$ GeV,
  - gamma-quark QED contribution [new !] leading at high P_T
  - gluon-fusion mostly dominant
  - $J/\psi + 2$ jets accessible
- $\sqrt{s_{ep}} = 45$ GeV,
  - gamma-quark QED contribution [new !] leading at high P_T

Conclusions

- For quarkonium production, QCD corrections with P_T-enhanced topologies are known to be important: we have revisited J/ψ photoproduction at HERA

- We have seen that CSM can describe the latest high-P_T HERA photoprod. data
- $\sqrt{s_{ep}} = 140$ GeV,
  - gamma-quark QED contribution [new !] leading at high P_T
  - gluon-fusion mostly dominant
  - $J/\psi + 2$ jets accessible
- $\sqrt{s_{ep}} = 45$ GeV,
  - gamma-quark QED contribution [new !] leading at high P_T

- We have also seen that QCD corrections are important for P_T-integrated σ.

Conclusions

- For quarkonium production, QCD corrections with P_T-enhanced topologies are known to be important: we have revisited J/ψ photoproduction at HERA

- We have seen that CSM can describe the latest high-P_T HERA photoprod. data
- $\sqrt{s_{ep}} = 140$ GeV,
  - gamma-quark QED contribution [new !] leading at high P_T
  - gluon-fusion mostly dominant
  - $J/\psi + 2$ jets accessible
- $\sqrt{s_{ep}} = 45$ GeV,
  - gamma-quark QED contribution [new !] leading at high P_T

- We have also seen that QCD corrections are important for P_T-integrated σ.

- We have identified a possible over subtraction of collinear divergences and employed a specific μ_F choice to avoid NLO negative σ at large $\sqrt{s_{\gamma p}}$

Conclusions

- For quarkonium production, QCD corrections with P_T-enhanced topologies are known to be important: we have revisited J/ψ photoproduction at HERA
- We have seen that CSM can describe the latest high-P_T HERA photoprod. data
- $\sqrt{s_{ep}} = 140$ GeV,
  - gamma-quark QED contribution [new !] leading at high P_T
  - gluon-fusion mostly dominant
  - $J/\psi + 2$ jets accessible
- $\sqrt{s_{ep}} = 45$ GeV,
  - gamma-quark QED contribution [new !] leading at high P_T
- We have also seen that QCD corrections are important for P_T-integrated σ.
- We have identified a possible over subtraction of collinear divergences and employed a specific μ_F choice to avoid NLO negative σ at large $\sqrt{s_{\gamma p}}$
- Loop correction matter and we anticipate significant NNLO corrections (likely positive) as well as a further reduction of the μ_R unc., esp. around 100 GeV

Conclusions

- For quarkonium production, QCD corrections with P_T-enhanced topologies are known to be important: we have revisited J/ψ photoproduction at HERA
- We have seen that CSM can describe the latest high-P_T HERA photoprod. data
- $\sqrt{s_{ep}} = 140$ GeV,
  - gamma-quark QED contribution [new !] leading at high P_T
  - gluon-fusion mostly dominant
  - $J/\psi + 2$ jets accessible
- $\sqrt{s_{ep}} = 45$ GeV,
  - gamma-quark QED contribution [new !] leading at high P_T
- We have also seen that QCD corrections are important for P_T-integrated σ.
- We have identified a possible over subtraction of collinear divergences and employed a specific μ_F choice to avoid NLO negative σ at large $\sqrt{s_{\gamma p}}$
- Loop correction matter and we anticipate significant NNLO corrections (likely positive) as well as a further reduction of the μ_R unc., esp. around 100 GeV
- This would likely allow us to better probe gluon PDFs.

Backup

Υ photoproduction

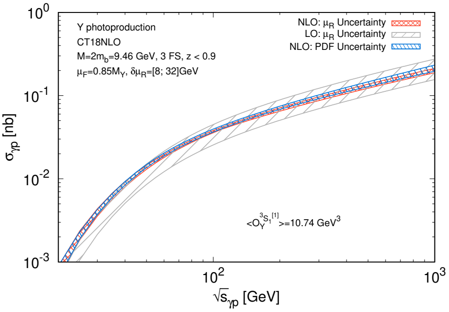

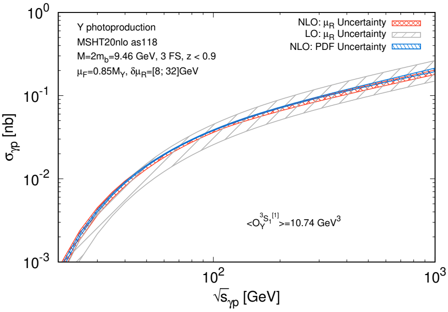

- We see further reduction of scale uncertainties at NLO comparably to LO

Υ photoproduction

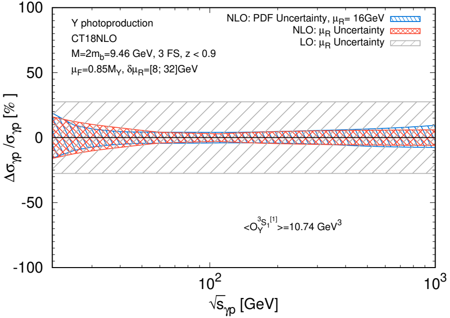

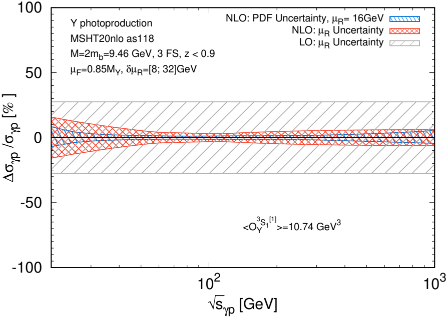

- We see further reduction of scale uncertainties at NLO comparably to LO
- PDF uncertainties are larger at high $\sqrt{s_{\gamma p}}$: a potential to probe PDFs

Dependence of $\sigma_{\gamma p}$ on the μ_R at an initial photon energy $s_{\gamma p}$

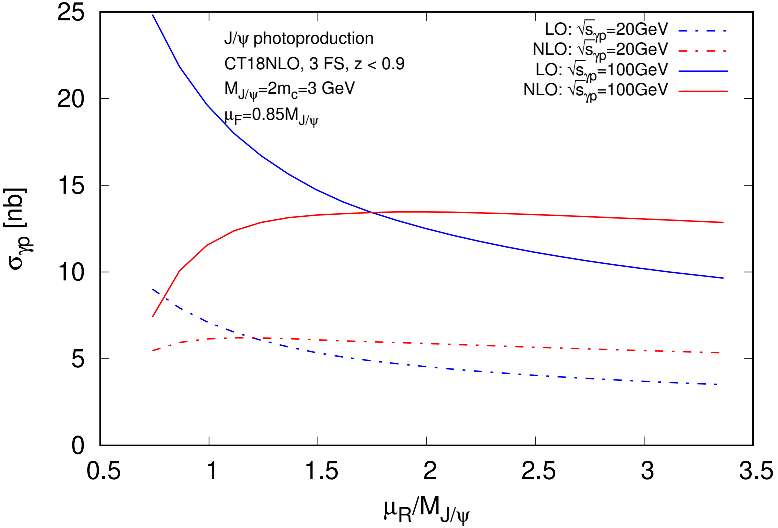

q& g contributions

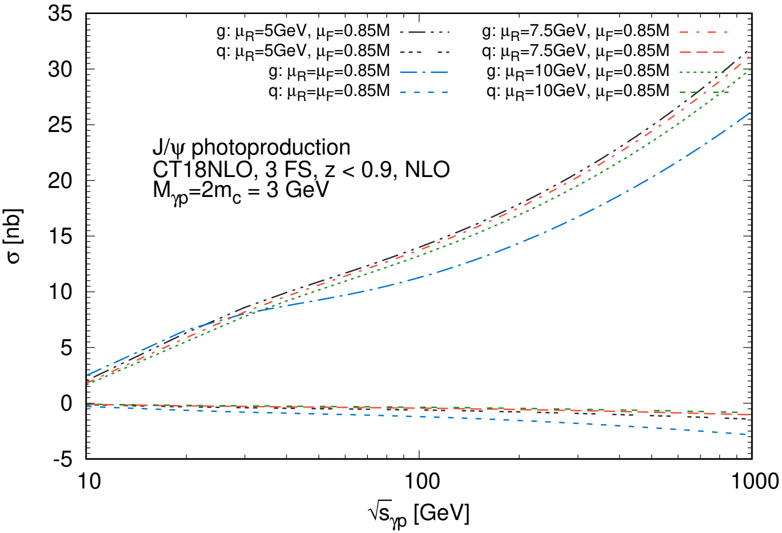

A scale prescription for μ_F

M.Krämer, NPB 459 (1996) 3-50

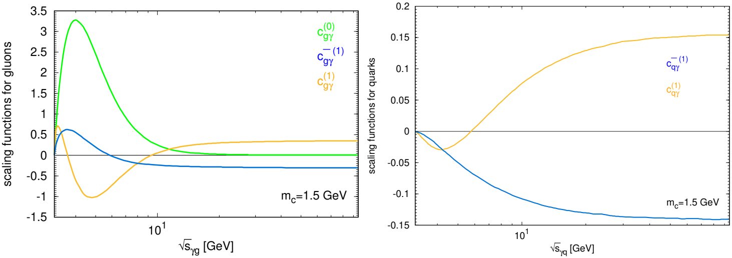

$$\hat{\sigma}_{i\gamma}(\hat{s},m_Q^2,\mu_R,\mu_F)=\frac{\alpha\alpha_s^2(\mu_R)e_Q^2}{m_Q^2}\,\frac{|R(0)|^2}{4\pi m_Q^3}\left[c^{(0)}_{g\gamma}(\hat{s},m_Q^2)+\right.$$

$$\left.+4\pi\alpha_s(\mu_R)\left\{c^{(1)}_{i\gamma}(\hat{s},m_Q^2)+\bar{c}^{(1)}_{i\gamma}(\hat{s},m_Q^2)\ln\frac{{\mu_F}^2}{m_Q^2}+\frac{\beta_0(n_{lf})}{8\pi^2}c^{(0)}_{g\gamma}(\hat{s},m_Q^2)\ln\frac{{\mu_R}^2}{{\mu_F}^2}\right\}\right]$$ (integrated over P_T and z)

$\lim_{\hat{s}\to\infty}\hat{\sigma}^{NLO}_{\gamma i}\propto\left(\log\frac{m_Q^2}{{\mu_F}^2}+A_{\gamma i}\right)$, where $A_{\gamma i}=-\frac{c^{(1)}_{i\gamma}(\hat{s},m_Q^2)}{\bar{c}^{(1)}_{i\gamma}(\hat{s},m_Q^2)}$, so $\hat{\mu}_F=M\exp\left(-\frac{c^{(1)}_{i\gamma}(\hat{s},m_Q^2)}{2\bar{c}^{(1)}_{i\gamma}(\hat{s},m_Q^2)}\right)$;

$\sigma(s_{\gamma p})\propto\sum_{i=q,g}\hat{\sigma}_{i\gamma}(\hat{s},\mu_F,\mu_R)\otimes f_i(x_i,\mu_F)$,

A scale prescription for μ_F

M.Krämer, NPB 459 (1996) 3-50

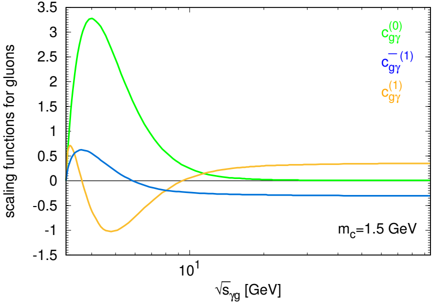

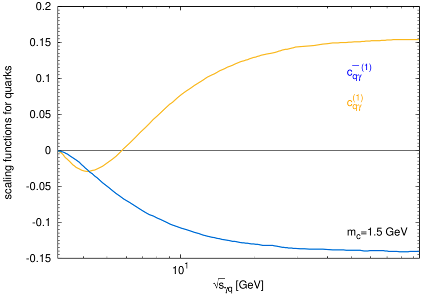

- Scaling functions for γg (γq) fusion, where $\hat{\sigma}_{i\gamma}$ were integrated over $z \leq 0.9$ and p_T.
- No light $q-$induced contributions at LO;
- 2 possible sources of negative partonic cross sections: loop corrections (interference) and from real emission
- flat PDFs can overemphasise the large $\hat{s}$ region

A scale prescription for μ_F: resummation

- Using Mellin transformation: $f(N) = \int_0^1 dx\, x^{N-1} f(x)$, we can rewrite $\hat{\sigma}$ from x to N space to in order to understand how the removal of these corrections which introduce negative σ works, and effectively corresponds to resummation of collinear emission contributions as an exponent;
- From the DGLAP equations we know that: $f(N, \hat{\mu}_F) \approx f(N, \mu_0) exp(\frac{2A\alpha_s(\mu_0)C_A}{\pi N})$, where we used $\gamma_{gg}(N) \approx \frac{2C_A}{N}$; $\alpha_s \neq \alpha_s(\mu)$, μ_0 is the default scale choice.
- In the exponent we did some approximate resummation for $\hat{s} \to \infty$: $\alpha_s^n \ln^{n-1} \frac{1}{\hat{z}} \to \frac{\alpha_s^n}{N^n}$ for $n = 0$, where $\hat{z} = \frac{M^2}{\hat{s}}$

μ_R choice

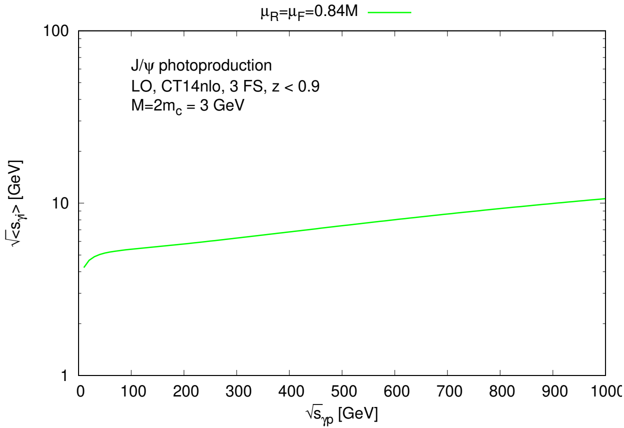

1. the natural scale choice in case of J/ψ photoproduction is not a mass of c-quark, becase of some loop corrections.
2. For J/ψ: $\mu_{Rmin} = 1.6m_c$ $(\sqrt{s_{\gamma p}} = 10\text{GeV})$

Full NLO for $P_T > 1$GeV

- With FDC code we obtained full NLO result;
- For $P_T > 1$GeV, $\sigma_{\gamma p} > 0$; the μ_F prescription was found for $P_T > 1$GeV

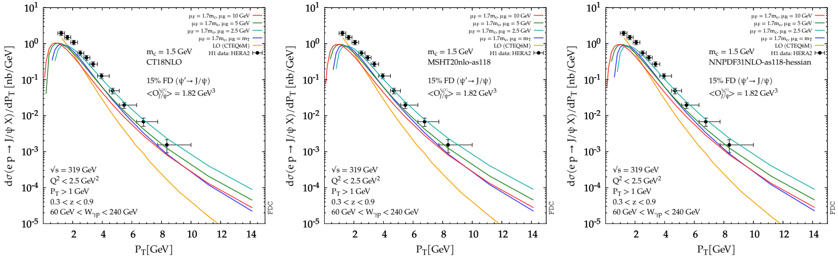

NLO*: P_T-discussion

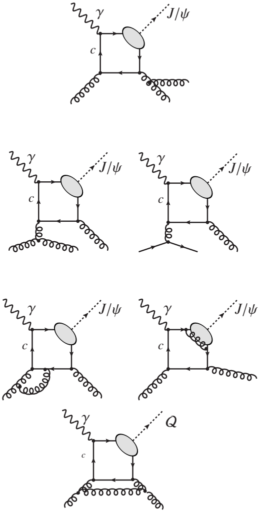

IR cut-off - a lower cut on the invariant mass of each pair of massless partons, s_{ij}.

$\ln(s_{ij}^{min})(1/p_T)^N$, $N \geq 8$

If the initial gluon/quark emits a large-p_T gluon/quark and if the final gluon is semi-hard, the increase of p_T results in the growth of all the possible $s_{ij} -> (1/p_T)^6$

We do not consider loop corrections in NLO*: $(1/p_T)^8$

Quarkonium Production Model

See Phys.Rept. 889 (2020) 1-106 and EPJC (2016) 76:107 for reviews

- No agreement on which mechanism is dominant
- Differences in the treatment of the hadronisation
- 3 common models:
  1. COLOUR SINGLET MODEL: hadronisation w/o gluon emission; colour and spin are preserved during the hadronisation
  2. NRQCD AND COLOUR OCTET MECHANISM: higher Fock states of the mesons taken into account; $Q\bar{Q}$ can be produced in octet states with different quantum # as the meson;
  3. COLOUR EVAPORATION MODEL: based on quark-hadron duality; only the invariant mass matters; semi-soft gluons emissions; colour-wise decorrelated $c\bar{c}$ prod. and hadr.

J/ψ+charm associated production at the EIC

C. Flore, J.P. Lansberg, H.S. Shao, YY, PLB 811 (2020) 135926

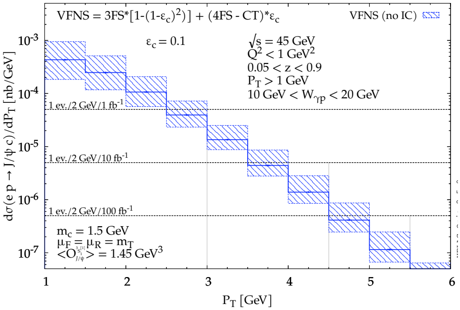

J/ψ+charm associated production at the EIC

C. Flore, J.P. Lansberg, H.S. Shao, YY, PLB 811 (2020) 135926

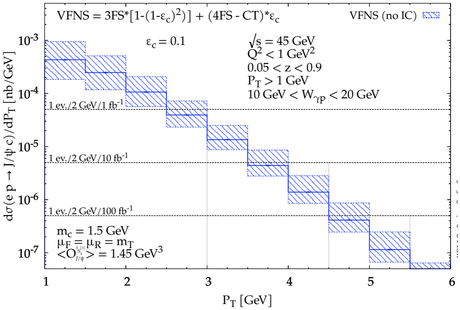

- Same LO VFNS computation previously shown in green except for the charm-detection efficiency ϵ_c: $VFNS =$ $3FS \times (1-(1-\epsilon)^2) + (4FS - CT) \times \epsilon$
- At $\sqrt{s_{ep}} = 45$ GeV, yield limited to low P_T even with $\mathcal{L} = 100\ \text{fb}^{-1}$
- But it is clearly observable if $\epsilon_c = 0.1$ with $\mathcal{O}(500, 50, 5)$ events for $\mathcal{L} = (100, 10, 1)\ \text{fb}^{-1}$

J/ψ+charm associated production at the EIC

C. Flore, J.P. Lansberg, H.S. Shao, YY, PLB 811 (2020) 135926

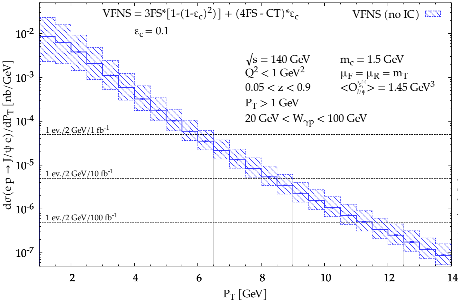

- Same LO VFNS computation previously shown in green except for the charm-detection efficiency ϵ_c: $VFNS =$ $3FS \times (1-(1-\epsilon)^2) + (4FS - CT) \times \epsilon$
- At $\sqrt{s_{ep}} = 45$ GeV, yield limited to low P_T even with $\mathcal{L} = 100$ fb^{-1}
- But it is clearly observable if $\epsilon_c = 0.1$ with $\mathcal{O}(500, 50, 5)$ events for $\mathcal{L} = (100, 10, 1)$ fb^{-1}
- At $\sqrt{s_{ep}} = 140$ GeV, P_T range up to 10 GeV with up to thousands of events with $\mathcal{L} = 100$ fb^{-1}
- Could be observed via charm jet

J/ψ+charm associated production at the EIC

C. Flore, J.P. Lansberg, H.S. Shao, YY, PLB 811 (2020) 135926

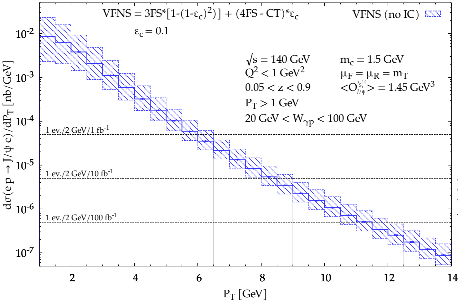

- Same LO VFNS computation previously shown in green except for the charm-detection efficiency ϵ_c: $VFNS =$ $3FS \times (1-(1-\epsilon)^2) + (4FS - CT) \times \epsilon$
- At $\sqrt{s_{ep}} = 45$ GeV, yield limited to low P_T even with $\mathcal{L} = 100$ fb^{-1}
- But it is clearly observable if $\epsilon_c = 0.1$ with $\mathcal{O}(500, 50, 5)$ events for $\mathcal{L} = (100, 10, 1)$ fb^{-1}
- At $\sqrt{s_{ep}} = 140$ GeV, P_T range up to 10 GeV with up to thousands of events with $\mathcal{L} = 100$ fb^{-1}
- Could be observed via charm jet

- 4FS $\gamma c \to J/\psi c$ depend on $c(x)$ and could be enhanced by intrinsic charm

J/ψ+charm associated production at the EIC

C. Flore, J.P. Lansberg, H.S. Shao, YY, PLB 811 (2020) 135926

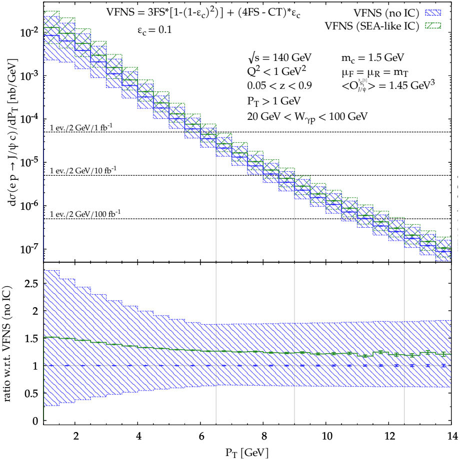

- Same LO VFNS computation previously shown in green except for the charm-detection efficiency ϵ_c: $VFNS =$ $3FS \times (1-(1-\epsilon)^2) + (4FS - CT) \times \epsilon$
- At $\sqrt{s_{ep}} = 45$ GeV, yield limited to low P_T even with $\mathcal{L} = 100$ fb^{-1}
- But it is clearly observable if $\epsilon_c = 0.1$ with $\mathcal{O}(500, 50, 5)$ events for $\mathcal{L} = (100, 10, 1)$ fb^{-1}
- At $\sqrt{s_{ep}} = 140$ GeV, P_T range up to 10 GeV with up to thousands of events with $\mathcal{L} = 100$ fb^{-1}
- Could be observed via charm jet

- 4FS $\gamma c \to J/\psi c$ depend on $c(x)$ and could be enhanced by intrinsic charm
- Small effect at $\sqrt{s_{ep}} = 140$ GeV [We used IC $c(x)$ encoded in CT14NNLO]

J/ψ+charm associated production at the EIC

C. Flore, J.P. Lansberg, H.S. Shao, YY, PLB 811 (2020) 135926

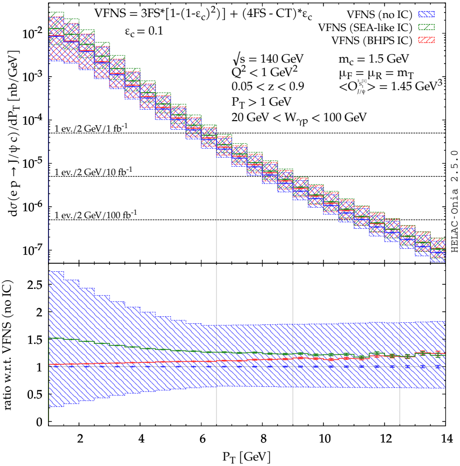

- Same LO VFNS computation previously shown in green except for the charm-detection efficiency

  ϵ_c: $VFNS =$

  $3FS \times (1-(1-\epsilon)^2) + (4FS - CT) \times \epsilon$
- At $\sqrt{s_{ep}} = 45$ GeV, yield limited to low P_T even with $\mathcal{L} = 100$ fb^{-1}
- But it is clearly observable if $\epsilon_c = 0.1$ with $\mathcal{O}(500, 50, 5)$ events for $\mathcal{L} = (100, 10, 1)$ fb^{-1}
- At $\sqrt{s_{ep}} = 140$ GeV, P_T range up to 10 GeV with up to thousands of events with $\mathcal{L} = 100$ fb^{-1}
- Could be observed via charm jet

- 4FS $\gamma c \to J/\psi c$ depend on $c(x)$ and could be enhanced by intrinsic charm
- Small effect at $\sqrt{s_{ep}} = 140$ GeV [We used IC $c(x)$ encoded in CT14NNLO]

J/ψ+charm associated production at the EIC

C. Flore, J.P. Lansberg, H.S. Shao, YY, PLB 811 (2020) 135926

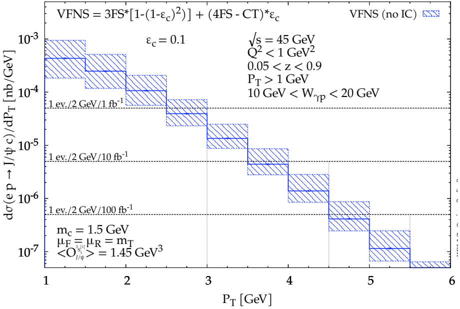

- Same LO VFNS computation previously shown in green except for the charm-detection efficiency ϵ_c: $VFNS =$ $3FS \times (1-(1-\epsilon)^2) + (4FS - CT) \times \epsilon$
- At $\sqrt{s_{ep}} = 45$ GeV, yield limited to low P_T even with $\mathcal{L} = 100$ fb^{-1}
- But it is clearly observable if $\epsilon_c = 0.1$ with $\mathcal{O}(500, 50, 5)$ events for $\mathcal{L} = (100, 10, 1)$ fb^{-1}
- At $\sqrt{s_{ep}} = 140$ GeV, P_T range up to 10 GeV with up to thousands of events with $\mathcal{L} = 100$ fb^{-1}
- Could be observed via charm jet

- 4FS $\gamma c \to J/\psi c$ depend on $c(x)$ and could be enhanced by intrinsic charm
- Small effect at $\sqrt{s_{ep}} = 140$ GeV [We used IC $c(x)$ encoded in CT14NNLO]
- Measurable effect at $\sqrt{s_{ep}} = 45$ GeV

J/ψ+charm associated production at the EIC

C. Flore, J.P. Lansberg, H.S. Shao, YY, PLB 811 (2020) 135926

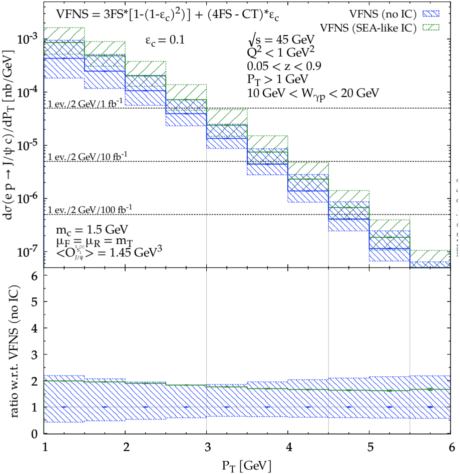

- Same LO VFNS computation previously shown in green except for the charm-detection efficiency ϵ_c: $VFNS = 3FS \times (1-(1-\epsilon)^2) + (4FS - CT) \times \epsilon$
- At $\sqrt{s_{ep}} = 45$ GeV, yield limited to low P_T even with $\mathcal{L} = 100$ fb^{-1}
- But it is clearly observable if $\epsilon_c = 0.1$ with $\mathcal{O}(500, 50, 5)$ events for $\mathcal{L} = (100, 10, 1)$ fb^{-1}
- At $\sqrt{s_{ep}} = 140$ GeV, P_T range up to 10 GeV with up to thousands of events with $\mathcal{L} = 100$ fb^{-1}
- Could be observed via charm jet

- 4FS $\gamma c \to J/\psi c$ depend on $c(x)$ and could be enhanced by intrinsic charm
- Small effect at $\sqrt{s_{ep}} = 140$ GeV [We used IC $c(x)$ encoded in CT14NNLO]
- Measurable effect at $\sqrt{s_{ep}} = 45$ GeV

J/ψ+charm associated production at the EIC

C. Flore, J.P. Lansberg, H.S. Shao, YY, PLB 811 (2020) 135926

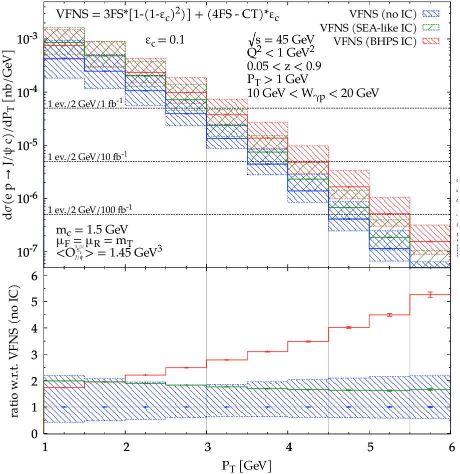

- Same LO VFNS computation previously shown in green except for the charm-detection efficiency ϵ_c: $VFNS =$ $3FS \times (1-(1-\epsilon)^2) + (4FS - CT) \times \epsilon$
- At $\sqrt{s_{ep}} = 45$ GeV, yield limited to low P_T even with $\mathcal{L} = 100$ fb^{-1}
- But it is clearly observable if $\epsilon_c = 0.1$ with $\mathcal{O}(500, 50, 5)$ events for $\mathcal{L} = (100, 10, 1)$ fb^{-1}
- At $\sqrt{s_{ep}} = 140$ GeV, P_T range up to 10 GeV with up to thousands of events with $\mathcal{L} = 100$ fb^{-1}
- Could be observed via charm jet

- 4FS $\gamma c \to J/\psi c$ depend on $c(x)$ and could be enhanced by intrinsic charm
- Small effect at $\sqrt{s_{ep}} = 140$ GeV [We used IC $c(x)$ encoded in CT14NNLO]
- Measurable effect at $\sqrt{s_{ep}} = 45$ GeV: BHPS valence-like peak visible !